Electronic Supplementary Material (ESI) for Physical Chemistry Chemical Physics.

Supplementary Information

Key Factors in Determining Arrangement of π Conjugated Oligomers inside Carbon Nanotubes

Takashi Yumura* and Hiroki Yamashita

Department of Chemistry and Materials Technology, Kyoto Institute of Technology, Matsugasaki, Sakyo-ku, Kyoto, 606-8585, Japan

S1. origin of interactions between the single terfuran and a nanotube host

S2. migration of an inner terfuran oligomer in 2×3F@(8,8) and 2×3F@(10,10)

S3. roles of the relative orientations of the cofacial terthiophene dimer in its energetics and optimal interchain spacings

S4. frontier orbitals based on multimeric terfurans in *n*×3F@(*m*,*m*)

S5. full lists in Ref. 53.

S1. Origin of interactions between the single terfuran and a nanotube host

Similar to single terthiophene oligomer inside an (*m*,*m*) nanotube (1×3T@(*m*,*m*)), we assume that host-guest interactions in 1×3F@(*m*,*m*) are due to π–π interactions and CH–π interactions. To verify this assumption, let us discuss the origin of interactions between a single methyl-terminated terfuran guest and a nanotube. Obtaining basic information on interactions between the 3F oligomer guest and the host tube, we discuss how methane interacts with benzene (motif I) as well as how furan interacts with naphthalene (motif II), as shown in Figure S1-1. Note that a single methyl-terminated terfuran consists of methyl groups and three furan rings and that benzene and naphthalene are one of the smallest fractions of a nanotube. Two motifs were considered for furan approaching the naphthalene (motifs IIa and IIb). In motifs I and IIa, the structures are stabilized by CH–π interactions, whereas π–π interactions are present in motif IIb. Thus, the key parameters in motifs I and IIa are separations between an H atom of CH_4 (furan, 1F) and a C atom of C_6H_6 (H(CH_4)···C(C_6H_6)) and those between an H atom of furan (1F) and a C atom of $C_{10}H_8$ (H(1F)···C($C_{10}H_8$)). Similarly, the distance between a C atom of furan and a C atom of naphthalene (C(1F)···C($C_{10}H_8$)) is a key parameter in motif IIb.

Figure S1-1a shows the potential energy for a methane approaching a benzene as a function of the H(CH_4)···C(C_6H_6) separation. Similarly, we see from Figures S1-1b and S1-1c potential energy surfaces for furan (1F) approaching to naphthalene according to the motifs IIa and IIb, respectively. In Figures S1-1b or S1-1c, the total

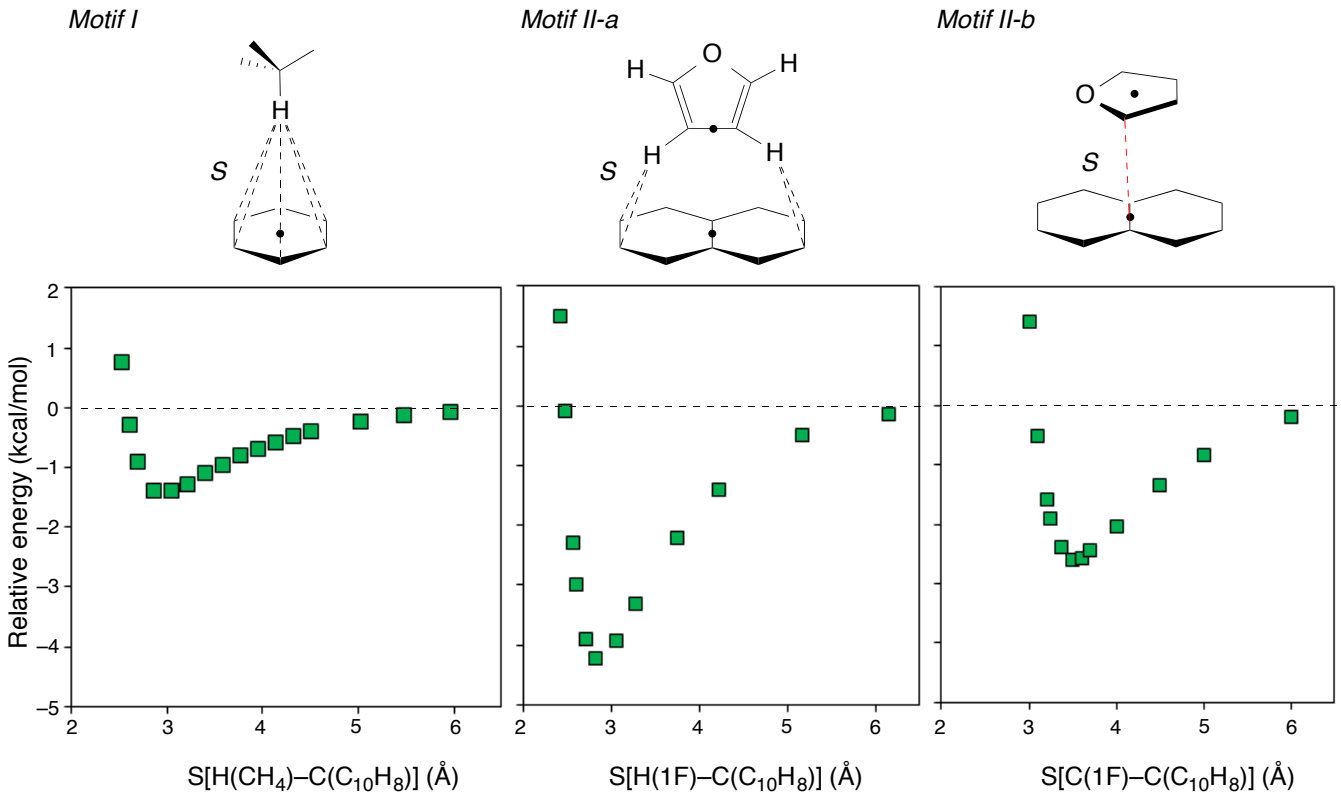

Fig S1-1 The potential surface (PES) for methane approaching to benzene (motif I), and those of furan (1F) approaching naphthalene (motifs II-a and II-b). The PES were obtained from the B97-D calculations. The energy values relative to the dissociation limit of furan and naphthalene are given. In motifs I and II-a, the structures are stabilized by CH–π interactions, whereas those in mofit II-b are stabilized by π–π interactions. Thus key parameters in motif I (II-a) are separation between an H atom of methane (1F) and a C atom of benzene (naphthalene), and those in motif II-b are separation between a C atom of 1F and a C atom of naphthalene.

energies of furan-naphthalene complexes are plotted as a function of the H(1F)···C($C_{10}H_8$) or C(1F)···C($C_{10}H_8$) separation.

First, examination of Figure S1-1 shows that each potential energy surface has one local minimum. The two important parameters characterizing each local minimum are listed in Table S1: the stabilization energy ($E_{stabilize}$) due to attractive methane-benzene or furan-naphtalene interactions, and their optimal separation (S_E). As shown in Figures S1-1b and S1-1c, furan-naphthalene complexes are stabilized by attractive CH–π and π–π interactions, with calculated magnitudes of 4.2 and 2.6 kcal/mol, respectively. The calculated S_E values in motifs IIa and IIb are 2.8 and 3.5 Å, respectively. Further approaching of furan into naphthalene for separation smaller than the S_E value leads to the destabilization of the complex. When the H(1F)···C($C_{10}H_8$) or C(1F)···C($C_{10}H_8$) separation is less than a certain value, the complex becomes energetically unstable relative to the dissociation limit. Here the separation where the complex is energetically identical to its dissociation limit is defined as S_0 in Table S1. Similarly, attractive CH–π interactions stabilize the methane-benzene complex at the H(CH_4)···C(C_6H_6) separation of 3.0 Å. The stabilization energy was calculated to be 1.4 kcal/mol. We also found the S_0 value in the methane-benzene complex. The $E_{stabilize}$, S_E, and S_0 values in Table S1 are similar to those in the thiophene-naphthalene complex, as discussed in Ref. 31.

Considering the basic information on the π–π interactions and CH–π interactions, we investigate the distribution of the internuclear separation for the guest and the tube

host in the 1×3F@(*m*,*m*) structures for distances ranging from 2.3 to 4.0 Å. Figure S1-2 shows the number of 0.1 Å internuclear separations between the single terfuran oligomer and a nanotube per unit interval. Three histograms are present in Figure S1-2, representing the separations of an oligomer H atom that is contained in a methyl or a furan ring from the C atoms of the tube (H(Me)···C(tube) or H(3F)···C(tube)) as well as those of the oligomer C atom from the tube C atom (C(3F)···C(tube)). The S_E and S_0 values in Table S1 are shown in the histograms by hashed and solid lines, respectively. Inspection of the histograms shows a substantial number of H(3F)···C(tube) and C(3F)···C(tube) contacts at approximately 2.8 and 3.5 Å, corresponding to the equilibrium separation in the furan-naphthalene complexes (S_E values). In addition, we did not find any H(3F)···C(tube) (C(3F)···C(tube)) contacts at the separation less than the S_0 value. These results indicate that the inner terfuran is stabilized by the attractive CH–π and π–π interactions between the inner wall of the tube.

Table S1 Key parameters in local minima of methane-benzene complex (motif I), and furan-naphthalene complexes (motifs II-a and II-b), as shown in Figure S1-1.

Key parameters	Methane-benzene complex (motif I)	Furan-naphthalene complex (motif II-a)	Furan-naphthalene complex (motif II-b)
$E_{stabilize}$ [d]	–1.4	–4.2	–2.6
S_{E} [e]	3.0	2.8	3.5
S_0	2.6	2.4	3.1

[a] $E_{\text{stabilize}}$ (kcal/mol): the stabilization energy in local minimum relative to its dissociation limit.
[b] S_E (Å): the optimal separation in a complex. H(CH_4)···C(C_6H_6) separation in motif I, H(1F)···C($C_{10}H_8$) separation in motif II-a, and C(1F)···C($C_{10}H_8$) separation in motif II-b.
[c] S_0 (Å): separation in a complex being energetically identical to its dissociation limit.

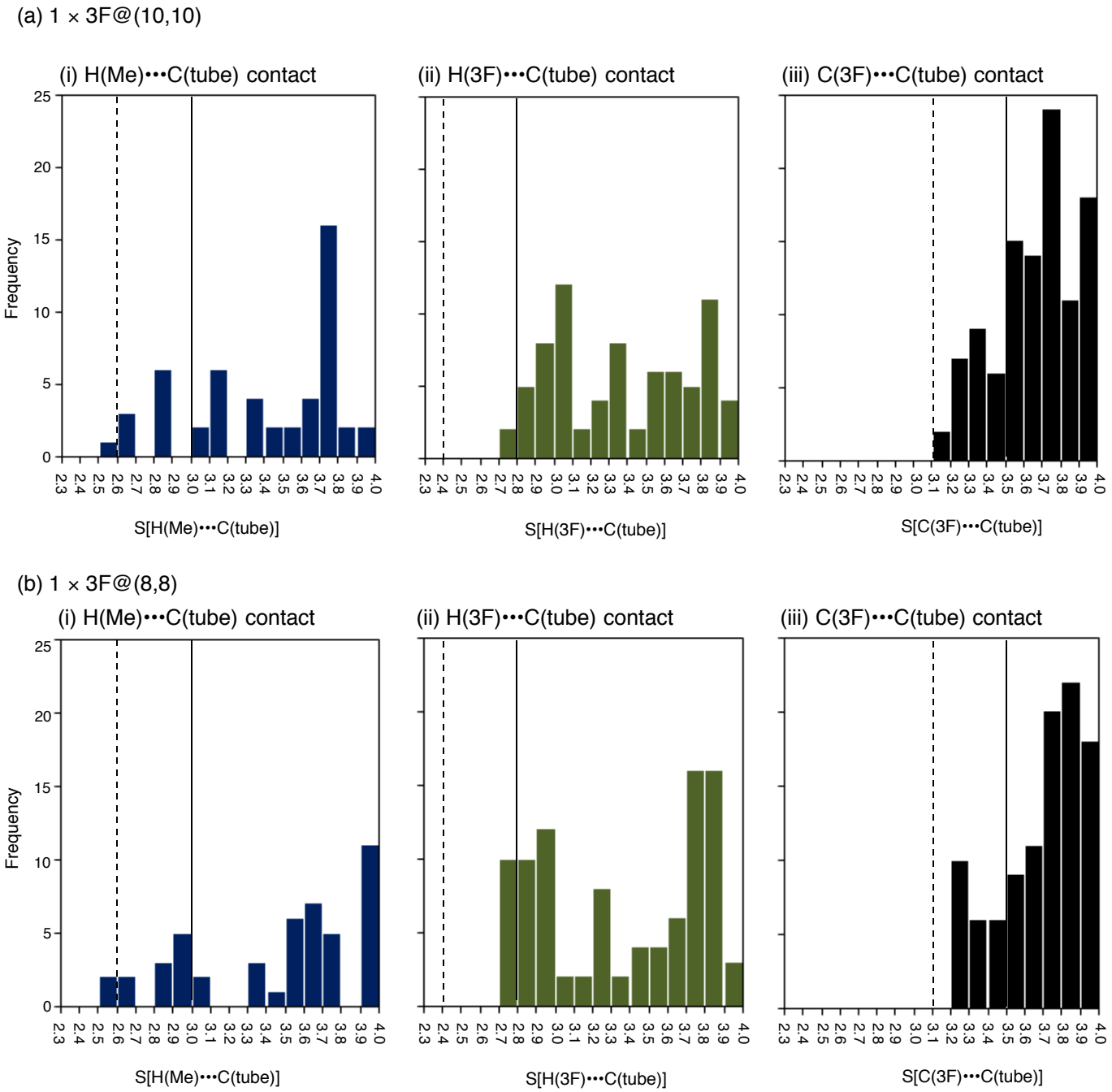

Fig. S1-2. Distribution of the internulear separations between the furan oligomer and the nanotube wall in the 1 × 3F@(*m*,*m*) obtained from B97D calculations. (i) Contact between a H atom of a methyl group and a carbon atom of the tube, (ii) contact between an H atom of a furan ring and a carbon atom of the tube, and (iii) contact between a C atom of a furan rings and a carbon atom of the tube. The S_E and S_0 values defined in Table S1 are displayed by hashed and solid lines, respectively.

S2. Migration of an inner terfuran oligomer in 2×3F@(8,8) and 2×3F@(10,10)

We investigated migration of an inner terfuran in 2×3F@(8,8) and 2×3F@(10,10), being similar to the single oligomer case (Figure 6). Figure S2 shows energy profiles of migration of an inner terfuran along the tube axis within the optimized 2×3F@(8,8) or optimized 2×3T@(10,10) (I) structure, obtained from B97-D calculations in Figure 7, and at the same time the other oligomer remained fixed at the original position. The degree of migration of the terfuran from its original position of an optimized structure is defined as M. Potential energy surface of the terfuran migration in 2×3F@(8,8) is given in Figure S2(I), and that in 2×3F@(10,10) is given in Figure S2(II). Inspection of Figure S2(II) shows that migration behaviors of an inner terfuran in 2×3F@(10,10) (I) are similar to those in 1×3F@(10,10) (Figure 6(II)) in terms of the energetics, because of the negligible interchain interactions in 2×3F@(10,10).

In contrast, there are substantial interchain interactions in 2×3F@(8,8). Then, the substantial interchain interactions in 2×3F@(8,8) significantly perturb the energy profile of migration of terfuran within the nanotube, differentiating 2×3F@(8,8) from 1×3F@(8,8) in terms of the migration behaviors. In fact, Figure S2(I) shows that the terfuran migration within 2×3F@(8,8) costs about 8 kcal/mol when *M* increases from 0 to 2.5 Å. The energy cost mainly comes from repulsion of methyl groups between the

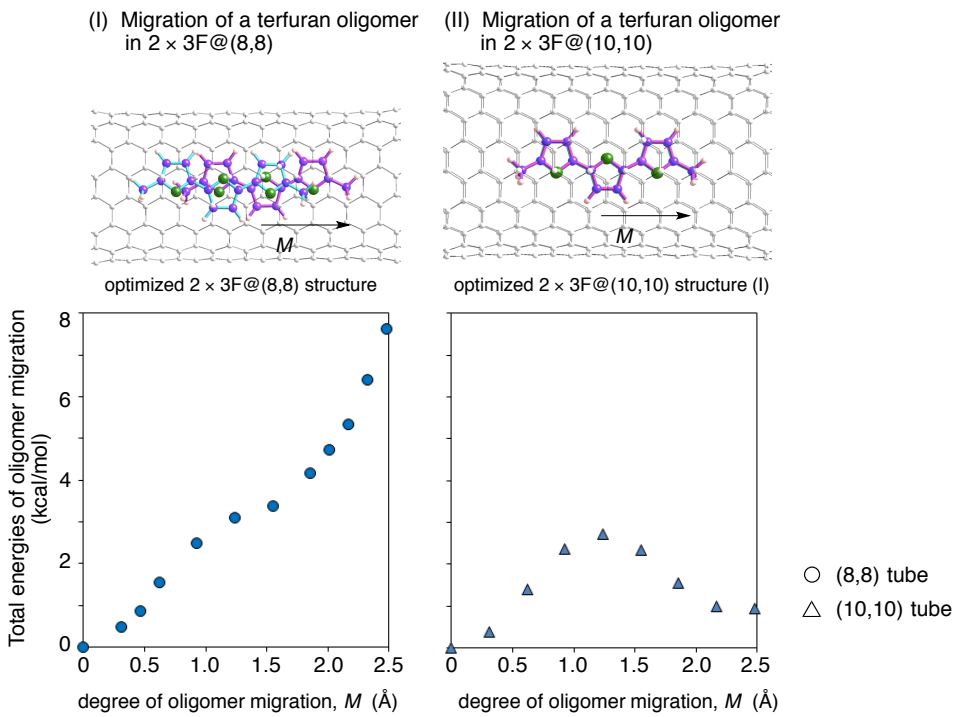

Fig. S2 Energy profiles of migration of an inner terfuran along the tube axis within an optimized 2 × 3F@(*m*,*m*) structure, obtained from B97-D calculations. The degree of migration on inner terfuran from its original position of an optimized structure is defined as *M*. Energies of terfuran migration in the inner spaces of the (8,8) and (10,10) tubes are give by cricles in (I) and triangles in (II), respectively.

two terfuran oligomers. Thus, the magnitude of interchain interactions can affect migration behaviors of a terfuran oligomer within 2×3F@(*m*,*m*) in terms of the energetics.

S3. Roles of the Relative Orientations of the Cofacial Terthiophene Dimer in Its Energetics and Optimal Interchain Spacings

Figure 8 shows cofacial-like arrangements of terfuran dimer inside an (8,8) nanotube; however, a terfuran slides from the original cofacial arrangement along the tube axis. Here, we investigate the impact of relative orientations of the cofacial terfuran dimers on the magnitude of their interchain interactions. As shown in Figure S3, we shifted one terfuran along the long axis (longitudinal shift,) from the original cofacial arrangement. At the same time, the other terfuran remained fixed at the original position. The longitudinal displacement is given by *y*(C). We plotted the total energy of the shifted terfuran dimers relative to the dissociation limit toward two terfurans ($E_{relative}$) as a function of the interchain spacing (z_{is}) in Figure S3. We find that there is one local minimum with respect to z_{is} in a relative orientation with a terfuran shifted longitudinally by a certain value (*y*(C)). Each local minimum is described by two key parameters: the stabilization energy (E_{min}) and the optimal

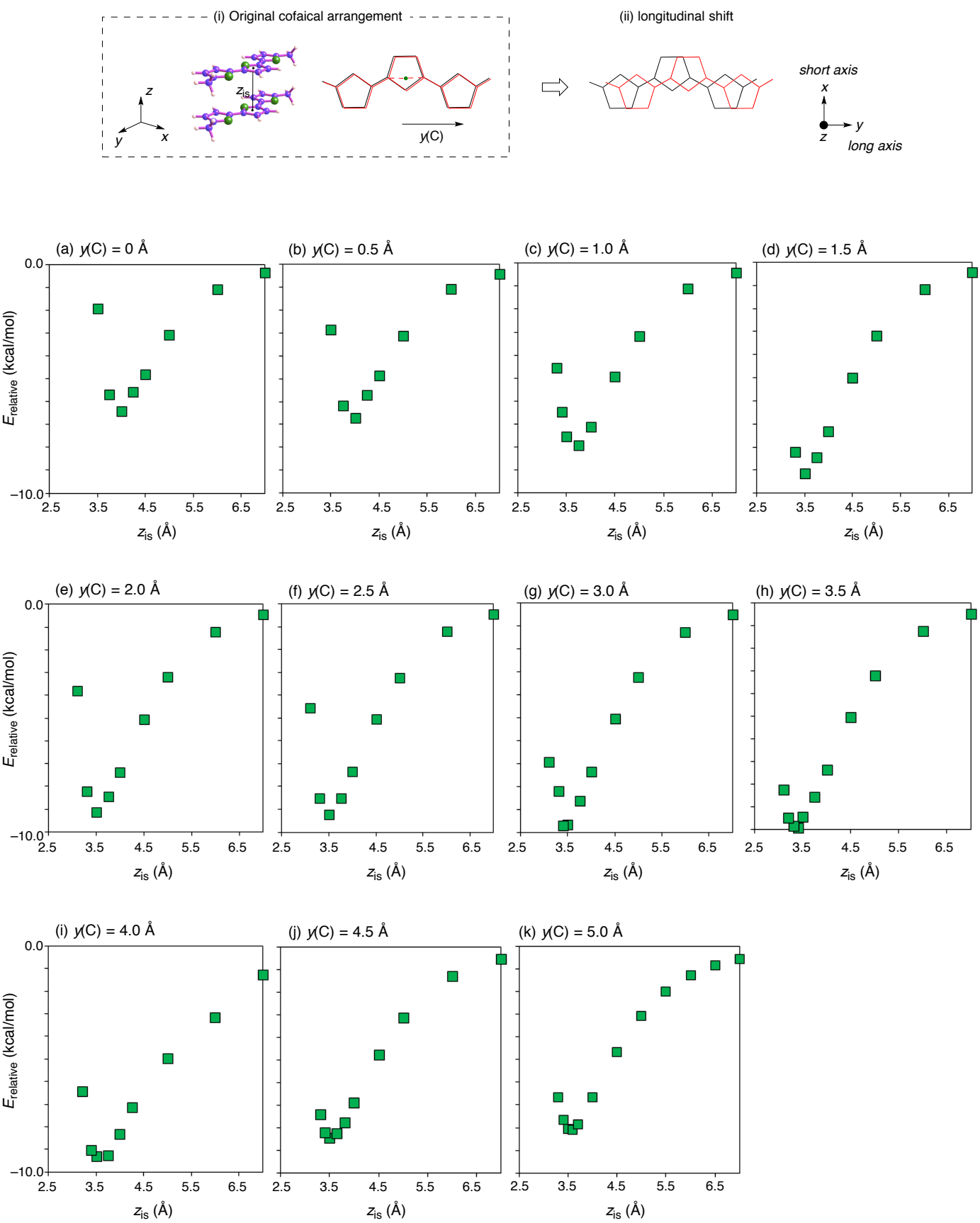

Fig. S3. Total energy changes of longitudinally-shifted terfuran dimers in cofacial fashion as a function of interchain spacing (z_{is}). The total energies of shifted cofacial dimers relative to the dissociation limit toward two terfurans ($E_{relative}$) are displayed. $E_{relative}$ values were obtained from B97D calculations. Values of y(C) correspond to displacement that one terfuran shifts longitudinally from the original cofacial arrangement. As shown in graphs, each potential energy surface (PES) has one local minimum whose stabilization energy (E_{min}). The E_{min} values depend on the displacements from original position y(C), displayed in Fig. 9.

interchain spacing. Figure S3 shows that the E_{min} values strongly depend on the y(C) values. We plotted the E_{min} values as a function of y(C) in Figure 9.

S4. Frontier orbitals Based on Multimeric Terfurans in *n*×3F@(*m*,*m*)

The different stacking arrangements in *n*×3F@(*m*,*m*) are responsible for the strengths of the interchain interactions and therefore play an important in determining the electronic properties of inner π-conjugated oligomers inside a nanotube and especially the splitting width of orbitals constructed from the frontier orbitals of the single oligomer, as shown in Figure S4a. Here, we focus on the splitting widths of the frontier orbitals of multimeric terfurans inside nanotubes. For example, orbitals in 2×3F@(8,8) constructed from the frontier orbitals of a single terfuran are given in Figure S4b. Figure S4b shows the orbitals with amplitudes located on the inner oligomers. The splitting width of the HOMO-built orbitals is 0.13 eV and that of the LUMO-constructed orbitals is 0.30 eV.

Table S4 lists the splitting widths of their frontier orbital-built orbitals in *n*×3F@(*m*,*m*). These values were obtained from B3LYP single point calculations of B97-D optimized *n*×3T@(*m*,*m*) structures. From the data in Table S4, we found that the splitting widths of the HOMO- or LUMO-constructed orbitals increase with increasing number of inner terfurans, as shown in Figure S4a. Significant increases in the splitting widths can be observed for the LUMO-constructed orbitals, rather than in the HOMO-constructed orbitals. In addition, we found different splitting widths of the

(a) Evolution of orbitals of multimeric terfuran chains

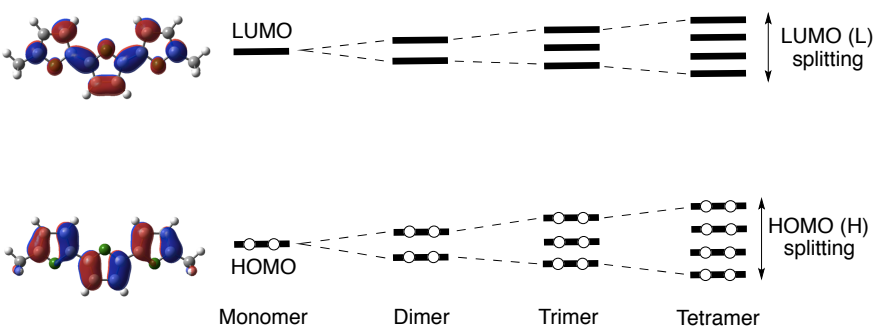

(b) Orbitals in 2 × 3F@(8,8) built from the HOMO or LUMO of a single terfuran chain.

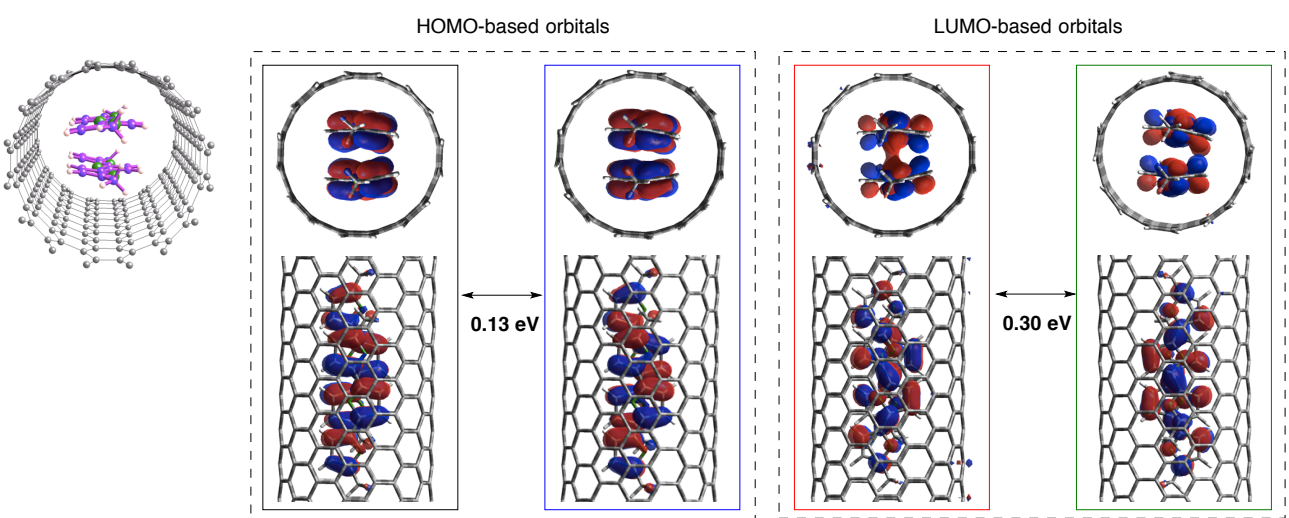

Fig S4. (a) Schematic view of the evolution of orbitals of multimeric terfuran chains, built from single-chain HOMO or LUMO. Orbital amplitudes of the HOMO and LUMO of a single terfuran chain are also given. (b) Features of orbitals built from multimeric terfurans of $2 \times 3F@(8,8)$ structures. Their orbital distributions were obtained from B3LYP-single point calculations of B97D optimized $2 \times 3F@(8,8)$ structures. B3LYP-obtained energies of orbitals built from inner terfuran guests, labeled by its orbital number, are given in parentheses.

HOMO- and LUMO-constructed orbitals of *n*×3F@(*m*,*m*) from those of *n*×3T@(*m*,*m*) (Ref. 32), clearly indicating different strengths of interchain interactions due to the different arrangements of the inner π-conjugated oligomers.

Table S4 Splittings of the orbitals of the multimeric terfurans surrounded by a nanotube (*n*×3T@(*m*,*m*)) are listed in eV. These values were obtained from B3LYP single point calculations of B97-D optimized *n*×3T@(*m*,*m*) structures.[a]

	(8,8)		(10,10)	
n [b]	Splitting of HOMO-built orbitals	Splitting of LUMO-built orbitals	Splitting of HOMO-built orbitals	Splitting of LUMO-built orbitals
2	0.13	0.30	0.02	0.12
3	0.38	0.43	0.07	0.18

[a] See detailed discussion and definition of splitting of HOMO- or LUMO-built orbitals of multimeric terfurans surrounded by an (*m*,*m*) nanotube.
[b] *n*: the number of terfurans contained in a nanotube.

S5. full lists in Ref. 53.

M. J. Frisch, G. W. Trucks, H. B. Schlegel, G. E. Scuseria, M. A. Robb, J. R. Cheeseman, G. Scalmani, V. Barone, B. Mennucci, G. A. Petersson, H. Nakatsuji, M. Caricato, X. Li, H. P. Hratchian, A. F. Izmaylov, J. Bloino, G. Zheng, J. L. Sonnenberg, M. Hada, M. Ehara, K. Toyota, R. Fukuda, J. Hasegawa, M. Ishida, T. Nakajima, Y.; Honda, O. Kitao, H. Nakai, T. Vreven, J. A., Jr. Montgomery, J. E. Peralta, F. Ogliaro, M. Bearpark, J. J. Heyd, E. Brothers, K. N. Kudin, V. N. Staroverov, R. Kobayashi, J. Normand, K. Raghavachari, A. Rendell, J. C. Burant, S. S. Iyengar, J. Tomasi, M. Cossi, N. Rega, J. M. Millam, M. Klene, J. E. Knox, J. B. Cross, V. Bakken, C. Adamo, J. Jaramillo, R. Gomperts, R. E. Stratmann, O. Yazyev, A. J. Austin, R. Cammi, C.

Pomelli, J. W. Ochterski, R. L. Martin, K. Morokuma, V. G. Zakrzewski, G. A. Voth, P. Salvador, J. J. Dannenberg, S. Dapprich, A. D. Daniels, Ö. Farkas, J. B. Foresman, J. V. Ortiz, J. Cioslowski and D. J. Fox, Gaussian 09, Gaussian, Inc.: Wallingford, CT, **2009**.